

Dissociation of CH₄ at High Pressures and Temperatures: Diamond Formation in Giant Planet Interiors?

Laura Robin Benedetti,¹ Jeffrey H. Nguyen,⁴
Wendell A. Caldwell,² Hongjian Liu,² Michael Kruger,⁵
Raymond Jeanloz^{2,3}

Experiments using laser-heated diamond anvil cells show that methane (CH₄) breaks down to form diamond at pressures between 10 and 50 gigapascals and temperatures of about 2000 to 3000 kelvin. Infrared absorption and Raman spectroscopy, along with x-ray diffraction, indicate the presence of polymeric hydrocarbons in addition to the diamond, which is in agreement with theoretical predictions. Dissociation of CH₄ at high pressures and temperatures can influence the energy budgets of planets containing substantial amounts of CH₄, water, and ammonia, such as Uranus and Neptune.

The luminosities and strong magnetic fields of the giant planets within the solar system require the presence of strong internal energy sources that are mainly primordial (resulting from gravitational collapse and internal differentiation, for instance). In addition to H₂ and He, Uranus and Neptune contain heavier molecular species such as methane (CH₄) (1); and because carbon is heavier than hydrogen, the chemical breakdown of CH₄ inside these planets—allowing carbon to sink—can affect their internal evolution and energetics (2–5). Such dissociation requires high temperature to break the C–H bonds (pyrolysis) and high pressure to condense the carbon. Motivated by recent theoretical predictions (5), we experimentally studied the stability of CH₄ under conditions like those existing inside Uranus and Neptune.

When heated at pressures and temperatures of 10 to 50 GPa and ~2000 to 3000 K (6), CH₄ exhibits a reaction creating two products, one opaque and the other transparent (Fig. 1). In situ x-ray diffraction, before and after heating, reveals the formation of diamond as a reaction product from the sample, not from the anvils (Fig. 2) (7). The occurrence of diamond is confirmed by micro-Raman spectroscopy on the opaque reaction product, quenched to zero pressure and removed from the diamond anvil cell (Fig. 2); the transparent reaction product and the unreacted CH₄ evaporate when pressure is released.

¹Department of Physics, ²Department of Geology and Geophysics, ³Department of Astronomy and Miller Institute for Basic Research in Science, University of California, Berkeley, CA 94720, USA. ⁴H-Division, Physics Directorate, Lawrence Livermore National Laboratory, Livermore, CA 94551, USA. ⁵Department of Physics, 4747 Troost, Room 227, University of Missouri, Kansas City, MO 64110, USA.

Diamond is not the only form of carbon present. Spatially resolved Raman spectra of both the opaque and transparent reaction products at high pressures exhibit vibrational modes that are characteristic of doubly and triply bonded carbon (Fig. 3). Moreover, we

can interpret the broad band evident in the Fourier-transform infrared absorption spectrum of the reacted sample as indicating that the CH₄ is partly polymerized upon reaction (Fig. 1) (8). The opaque reaction product does not contain hydrocarbon (C–H) bands, but the vibrational spectra of the transparent and opaque products do show that the intensity of the CH₄ peaks decreases upon reaction: The products are created at the expense of the reactant.

Hydrogen must be removed from CH₄ to form the carbon phases that are obtained as reaction products. We did not observe the Raman-active stretching mode of H₂ (9), but at pressures above 10 GPa we did find evidence of hydride forming in the rhenium gasket adjacent to the reactions (10). That it diffused into and reacted with the gasket provides indirect evidence that hydrogen is produced from the reacting CH₄. The presence of the rhenium gasket does not induce the dissociation of CH₄, however, as we were able to initiate the reaction away from the gasket with no evidence of disturbance across the surrounding unreacted CH₄ (10). Because this reaction is analogous to the formation of diamond from CH₄ by chemical vapor deposition at low pressures, it is plausible that the hydriding reaction inhibits the dissociation reactions (11).

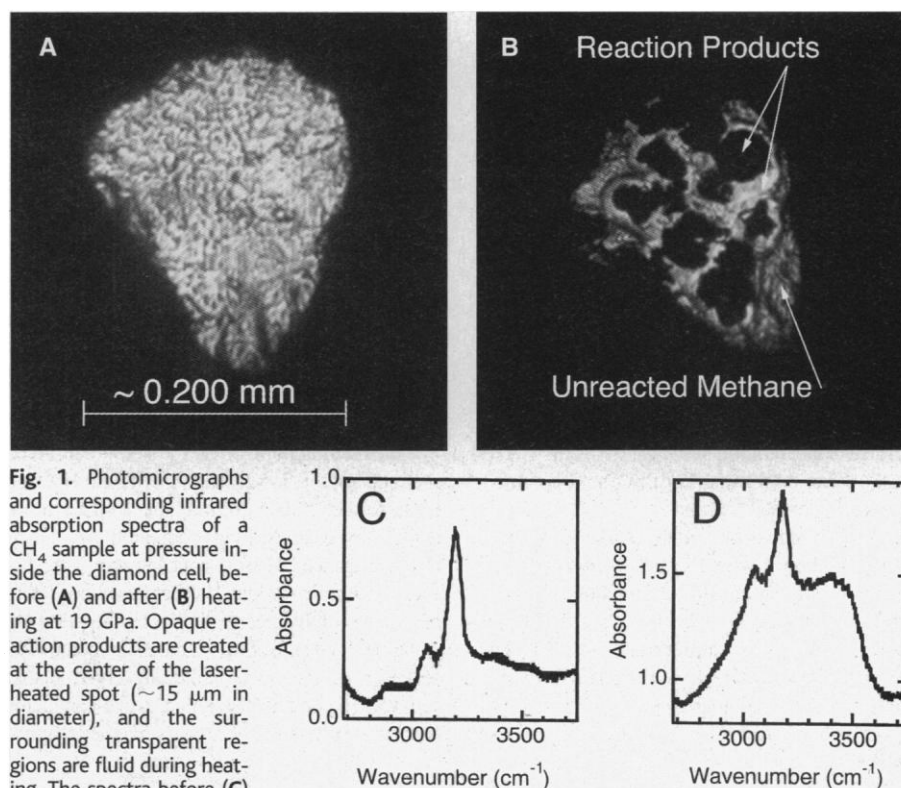


Fig. 1. Photomicrographs and corresponding infrared absorption spectra of a CH₄ sample at pressure inside the diamond cell, before (A) and after (B) heating at 19 GPa. Opaque reaction products are created at the center of the laser-heated spot (~15 μm in diameter), and the surrounding transparent regions are fluid during heating. The spectra before (C) and after (D) heating (23) show the 3050 and 3180 cm⁻¹ C–H vibrational modes characteristic of CH₄ decreasing in intensity relative to the background (24) and being replaced by a broad absorbance band (~3000 to 3400 cm⁻¹) characteristic of doubly and triply bonded carbon in hydrocarbons (8). Becke lines observed between the unreacted CH₄ and the transparent reaction product indicate a significantly higher index of refraction (hence, in all probability, density) for the product relative to the CH₄ (25).

We interpret the reaction induced in CH_4 at high pressures and temperatures as a partial chemical breakdown: $\text{CH}_4 \rightarrow (1-nx) \text{C} + n \text{C}_x\text{H}_y + (2-ny/2) \text{H}_2$, with the carbon (12) and hydrocarbon (C_xH_y) corresponding to the opaque and transparent reaction products observed in our experiments. Complete dissociation to pure carbon was only attained at the laser focus, in the center of the laser-heated spot; whereas partial breakdown to a mixture of variously polymerized hydrocarbons occurred in the cooler areas surrounding the hot spot. Higher temperatures (≥ 1500 to 2000 K) are apparently required to break all of the CH_4 bonds and form pure carbon, although the availability of nucleation sites for carbon condensation may also determine the local

degree of reaction within the sample (13).

Our experimental observations agree with the results of first-principles molecular dynamics simulations (5), which predict that CH_4 should dissociate to produce diamond at high pressures and temperatures. Moreover, the calculations indicate that hydrocarbon polymers of various lengths should be formed as precursors to this dissociation, just as indicated by our vibrational spectra. The main difference between the experimental and theoretical findings is in the pressure of the transformation: Theory suggests that CH_4 begins to break down and polymerize by 100 GPa and dissociates fully to form diamond only at pressures above 300 GPa, whereas we found that such a reaction proceeded at pressures as low as 10 to 20 GPa.

Fig. 2. Angle-dispersive x-ray diffraction patterns of a sample after heating to ~ 2000 K at 20 GPa. Unreacted CH_4 is observed (*) along with reaction products, including the two most intense diffraction peaks of diamond (diamonds). Additional lines are attributed to hydrocarbon reaction products (triangles), the ruby used for pressure calibration (circles), and iron from the gasket (squares) (strong intensities at 1.84 and 2.13 Å because of overlap with peaks from the reaction products and residual CH_4). (Inset) Raman spectrum (26) of the opaque reaction product at zero pressure, outside the diamond cell, showing the first-order vibrational mode of diamond at 1329 cm^{-1} . This Raman-active vibration differed slightly in frequency from that of natural diamond (1333 cm^{-1}) and had broad peaks (full width at half maximum ~ 7 to 8 cm^{-1}), probably due to the presence of lattice defects and internal stresses (27).

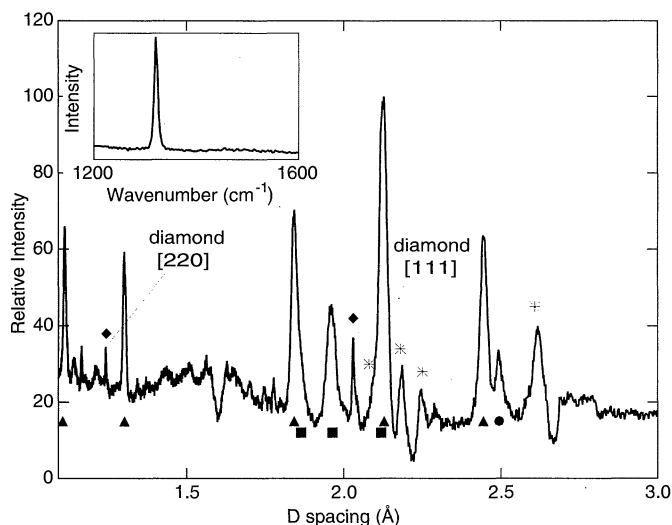
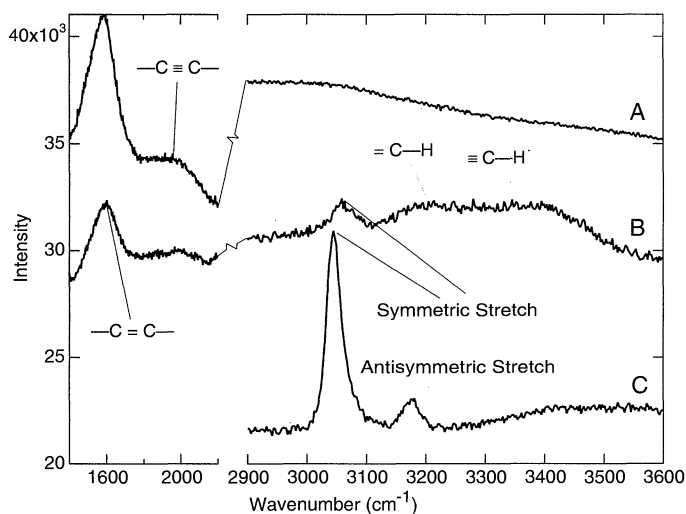


Fig. 3. In situ micro-Raman spectra of reaction products after heating at 19 GPa (note the break in scale between 2200 and 2900 cm^{-1}). At this pressure, frequencies of 3000 to 4000 cm^{-1} and 1600 to 2000 cm^{-1} are characteristic of the C-H bonds in hydrocarbons and of carbon bonding, respectively. The transparent reaction region (B) appears to contain more doubly and triply bonded hydrocarbons, whereas the opaque region (A) exhibits only carbon bond (not C-H) modes. The unreacted area of the sample (C) shows only the symmetric and antisymmetric CH_4 stretching vibrations, as in the sample before heating (Fig. 1), which indicates that no transformation has occurred.



The discrepancy may be artificial, however, in that the time scales of the molecular dynamics simulations are short (picoseconds) compared with those of the present experiments ($\sim 10^2$ to 10^3 s). Shock wave experiments, which probe an intermediate time scale (nanoseconds to microseconds), are interpreted in terms of CH_4 dissociation commencing above 40 to 50 GPa (2, 3).

Current models suggest that CH_4 accounts for 10 to 15% of Neptune's mass and resides primarily beneath its hydrogen-helium atmosphere at depths $\geq 10\%$ of Neptune's radius and at pressures ≥ 20 GPa (1). However, the experimental and theoretical results imply that chemical reactions and phase transformations among planetary molecular systems at high pressures and temperatures must be taken into account to model giant planet and brown dwarf (14) interiors more realistically. In particular, the energy released from gravitational settling of a carbon-rich phase such as diamond can contribute to internal heat sources, and hence interior dynamics, as well as to the externally observed luminosity and magnetic field (15). As more planets are found in unexpected orbits around other stars (16), the effects of internal chemical processes will need to be further clarified in order to obtain a general understanding of planet formation and evolution.

References and Notes

- W. B. Hubbard *et al.*, *Science* **253**, 648 (1991).
- M. Ross, *Nature* **292**, 435 (1981); F. H. Ree, *J. Chem. Phys.* **70**, 974 (1979).
- W. J. Nellis, F. H. Ree, M. van Thiel, A. C. Mitchell, *J. Chem. Phys.* **75**, 3055 (1981); H. B. Radousky, A. C. Mitchell, W. J. Nellis, *ibid.* **93**, 8235 (1990).
- S. Block, C. E. Weir, G. J. Piermarini, *Science* **169**, 586 (1970); R. H. Wentorf, *J. Phys. Chem.* **69**, 3063 (1965).
- F. Ancilotto, G. L. Chiarotti, S. Scandolo, E. Tosatti, *Science* **275**, 1288 (1997).
- CH_4 was heated and a reaction was observed at nine different pressures: 9, 10, 15, 19 (two times), 22, 30, 33, 37, and 47 GPa. Samples were cryogenically loaded as liquids into a Mao-Bell-type diamond cell, contained either with rhenium or steel gaskets, and then compressed at room temperature (17). Small (< 1 to $3 \mu\text{m}$) ruby grains (Cr^{3+} -doped Al_2O_3) were loaded with each sample to determine the pressure by the ruby fluorescence method (18), and platinum was included with some samples, both to serve as a pressure standard (by x-ray diffraction) and to enhance absorption of the laser beam used to heat the sample. Each sample was heated inside the diamond cell by means of the focused beam from a continuous Nd:YAG (Nd:yttrium-aluminum-garnet) laser, operated either in TEM₀₀ or multimode (19). Heating proceeded equally well with or without the presence of Pt (which did not appear to affect the observed reactions), plausibly because the 1064-nm wavelength of the Nd:YAG laser is close to the energy of the second overtone of the CH_4 stretching mode (Fig. 1). Samples initially absorbed the laser beam strongly, but the absorption decreased as the reaction proceeded (which is consistent with our inference that the CH_4 was directly absorbing the laser energy). Although the time-varying heating of the reacting sample precluded our making accurate temperature measurements by spectroradiometry, peak temperatures during the reaction were visually estimated to be in the range of 2000 to 3000 K, judging from the color and intensity of the hot spot in comparison

- with those of steady hot spots for which spectroradiometry was possible. There was no evidence of any reaction without heating.
7. Angular-dispersive x-ray patterns were obtained at Stanford Synchrotron Radiation Laboratory beamline 10-2, using image plates with 17.038-keV monochromatic radiation. The patterns were analyzed as described by J. H. Nguyen and R. Jeanloz [*Rev. Sci. Instrum.* **64**, 3456 (1993)]. The diffraction rings ascribed to diamond were narrow and uniform in intensity, indicating a randomly oriented polycrystalline reaction product and not diffraction from the single-crystal diamond anvils or chips coming off the anvils (which would instead yield individual diffraction spots or spotty diffraction rings). Additionally, there was no evidence after the experiments of any damage to the diamond anvils that could account for the evidence that diamond was present within the reacted samples.
 8. Alkenes and alkynes, containing doubly and triply bonded carbons, are characterized by C-H stretching frequencies shifted upward by ~ 100 to 200 cm^{-1} and another ~ 200 to 300 cm^{-1} relative to those of singly bonded alkanes and CH_4 [D. C. Harris and M. D. Bertolucci, *Symmetry and Spectroscopy* (Dover Publications, New York, 1978)]. The vibrational frequencies depend on the types of bonds present and on the size and orientation of the molecule. The broad absorption band observed after reaction is therefore best interpreted as a superposition of bands from a mixture of differently sized and bonded hydrocarbons.
 9. It is possible that hydrogen was present, but our Raman data near the H_2 vibrational mode at $\sim 4250\text{ cm}^{-1}$ [P. Loubeyre *et al.*, *Nature* **383**, 702 (1996)] were consistently too noisy to allow a definitive identification. Molecular hydrogen (H_2) exhibits no first-order infrared absorption, and free atomic hydrogen (H) has neither an infrared nor a Raman signature.
 10. L. R. Benedetti and R. Jeanloz, in preparation. An x-ray beam collimated to a diameter of $20\text{ }\mu\text{m}$ was used to collect spatially resolved x-ray diffraction patterns at National Synchrotron Light Source beamline X17c. Energy dispersive patterns collected at $2\theta = 10^\circ$ documented an expanded unit cell for the part of the rhenium gasket adjacent to reaction products, and not for the part of the gasket next to unheated portions of the sample or in regions away from the sample. The observed shifts in lattice parameters, amounting to an expansion of as much as 2.6% ($\pm 0.2\%$), are characteristic of rhenium hydride formation, with values of x up to 0.18 in ReH_x (20). Also, although iron hydride is formed more easily under pressure than is rhenium hydride (20, 21), we found no difference in results between samples contained in iron gaskets and those in rhenium gaskets.
 11. J. C. Angus *et al.*, *Philos. Trans. R. Soc. London Ser. A* **342**, 195 (1993); C.-P. Klages, *Appl. Phys. A (Solids Surf.)* **A56**, 513 (1993). Diamond formed by chemical vapor deposition is extracted from CH_4 through a complex series of reactions that are chemically and structurally reliant on the presence of free hydrogen. If the process we observed is similar, then as hydrogen diffuses into the gasket, less hydrogen is available to sustain the diamond-forming reaction that we observed.
 12. In addition to diamond, as described in the text, Raman spectroscopy of the opaque reaction product indicates the presence of varying amounts of another carbon phase that we infer to be amorphous carbon because it produces no identifiable x-ray diffraction lines.
 13. Sample regions with more ruby appeared to form more reaction products, which suggests that the ruby used for pressure calibration may provide nucleation sites. Also, Raman spectra of recovered material outside the diamond anvil cell indicate that the carbonaceous (opaque) reaction product was generally attached to ruby grains. Yoshimoto *et al.* similarly observed that Al_2O_3 provided nucleation sites for diamond growth (22). We did not observe any evidence of chemical reaction between the CH_4 and ruby, however, as the intensities of the fluorescence and x-ray diffraction lines of ruby were unchanged (within our resolution) before and after heating.
 14. B. R. Oppenheimer, S. R. Kulkarni, K. Matthews, M. H. van Kerkwijk, *Astrophys. J.* **502**, 932 (1998); J. Liebert and W. B. Hubbard, *Nature* **400**, 316 (1999).
 15. An estimate of the energy that can be released from a dissociation reaction was made by calculating the gravitational energy for two models of Neptune's interior. The first is a three-layer model (rocky core, molecular "ice" layer, and hydrogen-helium atmosphere) by Hubbard (7), and the second is the same model except that the CH_4 in the "ice" layer is dissociated into diamond and hydrogen, with the diamond located at the bottom of the layer and the hydrogen at the top. The energy difference of $1.1 \times 10^{33}\text{ J}$ that is released in going from the first model to the second can be a significant source of internal energy for the planet. For comparison, Neptune is observed to radiate more than twice the energy it receives from the sun; the excess, $3.2 \times 10^{15}\text{ W}$, must be produced internally and corresponds to $0.45 \times 10^{33}\text{ J}$ over the 4.5-billion-year age of the solar system.
 16. R. P. Butler *et al.*, in preparation.
 17. H. K. Mao, P. M. Bell, K. J. Dunn, R. M. Chrenko, R. C. DeVries, *Rev. Sci. Instrum.* **50**, 1002 (1979).
 18. H. K. Mao *et al.*, *J. Appl. Phys.* **49**, 3276 (1978).
 19. R. Jeanloz and A. Kavner, *Philos. Trans. R. Soc. London Ser. A*, **354**, 1279 (1996); A. Kavner and R. Jeanloz, *J. Appl. Phys.* **83**, 7553 (1998).
 20. T. Atou and J. V. Badding, *J. Solid State Chem.* **118**, 299 (1995). Atou and Badding observed rhenium hydride with a stoichiometry up to $x = 0.38$ for ReH_x .
 21. J. V. Badding and R. J. Hemley, *Science* **253**, 412 (1991).
 22. M. Yoshimoto *et al.*, *Nature*. **399**, 340 (1999).
 23. Infrared absorbance spectra (at 2 cm^{-1} resolution) were recorded with a Bruker IFS66v Fourier-transform spectrometer using a Globar (mid-infrared) source, a calcium fluoride (CaF_2) beamsplitter, and a liquid N_2 -cooled InSb detector.
 24. R. Bini and G. Pratesi, *Phys. Rev. B* **55**, 14800 (1997); Y. H. Wu, S. Sasaki, H. Shimizu, *J. Raman Spectrosc.* **26**, 963 (1995). The CH_4 molecule has four normal modes of oscillation: a symmetric stretch, an antisymmetric stretch, a symmetric deformation, and an antisymmetric deformation. The vibrational frequencies of these modes are, respectively, 2917 cm^{-1} , 3019 cm^{-1} , 1534 cm^{-1} , and 1306 cm^{-1} at ambient pressure and temperature, and they increase as pressure is raised (temperature is expected to have only a secondary effect).
 25. F. D. Bloss, *An Introduction to the Methods of Optical Crystallography* (Holt, Rinehart & Winston, San Francisco, 1961).
 26. Raman spectra were excited with a Lexel 95 argon-ion laser tuned to a wavelength of 514.5 nm and were collected through a triple grating monochromator/spectrograph (Spectra Pro 750) to a liquid N_2 -cooled charge-coupled device detector (Princeton Instruments ST 138, 100×1340 pixels). The laser was focused through a microscope, allowing 3 cm^{-1} spectral resolution within a $\sim 5\text{-}\mu\text{m}$ spot.
 27. J. Michler *et al.*, *J. Appl. Phys.* **83**, 187 (1998).
 28. We thank P. Alivisatos, K. Jacobs, W. Panero, H. Scott, and S. Zelman for experimental support and helpful discussions. Supported by NSF and NASA.

10 June 1999; accepted 20 August 1999

Laminar Ceramics That Exhibit a Threshold Strength

M. P. Rao,¹ A. J. Sánchez-Herencia,^{1*} G. E. Beltz,²
R. M. McMeeking,^{1,2} F. F. Lange^{1†}

Thin compressive layers within a laminar ceramic arrest large cracks (surface and internal) and produce a threshold strength. This phenomenon increases the damage tolerance of ceramics and will allow engineers to design reliable ceramic components for structural applications. The stress intensity factor derived for a crack sandwiched between two compressive layers suggests that the threshold strength is proportional to the residual compressive stress and the thickness of the compressive layer and is inversely proportional to the distance between the compressive layers. Laminates composed of thick alumina layers (605 ± 11 micrometers) and thin mullite/alumina compressive layers (37 ± 1.4 micrometers) fabricated for this study had a threshold strength of 482 ± 20 megapascals, in fair agreement with the theory.

The strength of brittle materials, including ceramics and glasses, must be described by statistical parameters (such as those of Weibull) because they contain an unknown variety of cracks and cracklike flaws that are inadvertently introduced during processing and surface machining (1, 2). Typical flaws found at fracture origins include large voids produced by organic inclusions (such as a human hair) and inorganic inclusions (such as

a dust particle or agglomerated particles). These flaws originate in the ceramic powders used to make the components. Failure from these types of flaws is generally not an issue in ductile materials, such as metals, because they exhibit plastic deformation that desensitizes the relation between small flaws and strength. Plastic deformation also absorbs work from the loading system to increase the metal's resistance to the extension of large cracks. However, the lack of plastic deformation causes the strength of ceramics to be inversely dependent on the size of very small cracks, which generally cannot be detected except by failure itself. For this reason, a specific ceramic component could exhibit a high probability of failure.

¹Materials Department, ²Department of Mechanical and Environmental Engineering, University of California at Santa Barbara, Santa Barbara, CA 93106, USA.

*Present address: Instituto de Cerámica y Vidrio (CSIC), Arganda del Rey, 28500 Madrid, Spain.

†To whom correspondence should be addressed.